

Iridium and Rhodium Complexes within a Macroreticular Acidic Resin: A Heterogeneous Photocatalyst for Visible-light Driven H₂ Production without an Electron Mediator

Kohsuke Mori,^{*[a, b]} Yoshihiko Kubota,^[a] and Hiromi Yamashita^{*[a, b]}

Abstract: Direct ion exchange of cyclometalated iridium(III) and tris-2,2'-bipyridyl rhodium(III) complexes, of which the former acts as a photosensitizer and the latter as a proton reduction catalyst, within a macroreticular acidic resin has been accomplished with the aim of developing a photocatalyst for H₂ production under visible-light irradiation. Ir L_{III}-edge and Rh K-edge X-ray absorption fine structure (XAFS) measurements suggest that the Ir and Rh complexes are easily accommodated in the macroreticular space

without considerable structural changes. The photoluminescence emission of the exchanged Ir complex due to a triplet ligand charge-transfer (³LC) and metal-to-ligand charge-transfer (³MLCT) transition near 550 nm decreases with increasing the amount of the Rh complex, thus suggesting the occurrence of an electron transfer from

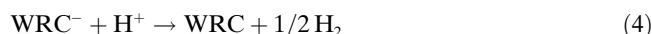
Keywords: ion exchange • iridium • H₂ production • photocatalysis • rhodium

Ir to Rh. The Ir-Rh/resin catalyst behaves as a heterogeneous photocatalyst capable of both visible-light sensitization and H₂ production in an aqueous medium in the absence of an electron mediator. The photocatalytic activity is strongly dependent on the amount of the components and reaches a maximum at a molar ratio of 2:1 of Ir/Rh complexes. Moreover, leaching and agglomeration of the active metal complexes are not observed, and the recovered photocatalyst can be recycled without loss in catalytic activity.

Introduction

The exploitation of a H₂ production system driven by visible light irradiation in an aqueous medium has been strongly desired in the effort towards environmentally friendly artificial photosynthetic methods.^[1] A variety of heterogeneous systems based on semiconducting metal oxides, exemplified by TiO₂, have been examined for water splitting into H₂ and O₂ since the late 1970s,^[2] and considerable achievements have been attained.^[3] On the other hand, molecular-based photosystems in homogeneous solutions have also been actively studied in recent years for photoinduced H₂ production.^[4] The molecular-based photocatalytic systems generally involve multiple components including a photosensitizer (PS) responsible for the absorption of visible light in conjunction with an electron relay (ER) that quenches the excited photosensitizer through electron transfer and a water

reduction catalyst (WRC) to produce H₂ and sacrificial reagents (SRs), thus providing the electron replenishing the lowest singly occupied molecular orbital of the PS⁺. The overall reaction is considered as a visible light-driven proton reduction process by SR to molecular hydrogen via electron relay according to Equation (1)–(5).



Historically, [Ru(bpy)₃]²⁺ (bpy = 2,2'-bipyridine) has been most commonly used as a PS and methyl viologen (MV²⁺) has been frequently employed as an ER.^[5] In order to remove toxic and expensive MV²⁺ from the reaction mixture, continuous efforts have also been devoted to construct organized multinuclear systems comprising a [Ru(bpy)₃]²⁺-derived PS component and a Pt^{II}-based H₂-evolving component.^[4d,6] The next evolution step is the use of cyclometalated Ir^{III} complexes as a sensitizer.^[7] These complexes exhibit longer excited-state lifetimes compared to the Ru analogues and are capable of direct electron transfer to the reducing species, such as Pt colloids, [Co(bpy)₃]²⁺, and [Rh(bpy)₃]³⁺, with better quantum yields. However, the use of such metal

[a] Dr. K. Mori, Y. Kubota, Prof. Dr. H. Yamashita
Graduate School of Engineering
Osaka University
1-2 Yamadaoka, Suita, Osaka 565-0871 (Japan)
Tel/Fax: (+81)6-6879-7460
Tel/Fax: (+81)6-6879-7457
E-mail: mori@mat.eng.osaka-u.ac.jp
yamashita@mat.eng.osaka-u.ac.jp

[b] Dr. K. Mori, Prof. Dr. H. Yamashita
Unit of Elements Strategy Initiative for Catalysts & Batteries
Kyoto University
Katsura, Kyoto 615-8520 (Japan)

complexes on an industrial scale would lead to practical problems due to large amounts of organic solvents needed, and difficulties in recovering the expensive transition metals and ligands and in separating the products.

Ion-exchange resins have been extensively employed in fundamental academic and industrial works.^[8] The unique characteristics of such resins, including acid/base as well as hydrophilic/hydrophobic properties, the ease of the introduction of a wide variety of functional groups, and their ability to swell in a reaction medium, make these materials very attractive from the viewpoint of catalyst design.^[9] Moreover, these resins can be utilized to stabilize metal complexes and highly dispersed metal nanoparticles (NPs) inside macroreticular domains with controllable morphology, accompanied with rational thermal and mechanical stability, thus affording a promising catalyst support for industrial applications. It is well accepted that the existence of suitable surface functional groups in the vicinity of active metal centers exerts a positive influence on catalytic activity. Additionally, swelling properties can result in dramatic improvements in the accessibility of reactants in the liquid phase. Consequently, catalytically active species entrapped within functional resin matrices fundamentally differ from conventional metal catalysts supported on solid inorganic materials.^[10]

In this paper, we present a new photocatalyst created by simple ion exchange of the bis-(2-phenylpyridine)-(2,2'-bipyridine)iridium (III) ($[\text{Ir}(\text{ppy})_2(\text{bpy})]^+$) complex and tris-2,2'-bipyridyl rhodium(III) ($[\text{Rh}(\text{bpy})_3]^{3+}$) on a cation-exchange resin possessing strongly acidic $-\text{SO}_3^-$ groups within its macroreticular matrix (Figure 1). Recently, Ir^{III} complexes have been the subject of numerous studies with

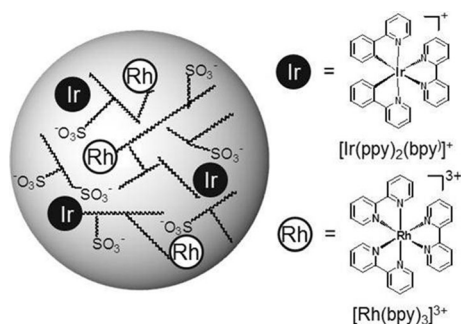


Figure 1. Schematic illustration of the acidic resin after ion exchange with Ir and Rh complexes.

regard to their application in electrophosphorescent organic light-emitting diodes (OLEDs).^[11] It can be envisaged that Ir^{III} complexes could be promising photosensitizers that successfully promote the electron transfer from the $^3\text{MLCT}$ state (MLCT = metal-to-ligand charge-transfer) to proton reduction catalysts owing to their unprecedented high luminescence quantum yield (~ 1) originating from their high ligand field splitting. $[\text{Rh}(\text{bpy})_3]^{3+}$ is an ideal candidate for the proton reduction catalyst component because it accumulates two electrons at a suitable potential for H_2 production

and is known to form hydrides.^[12] Herein, it is proven that the introduction of both Ir and Rh complexes enables H_2 production in aqueous media without an electron relay by visible-light photosensitization. We also investigated the effects of functional groups, loading amount, as well as reaction conditions.

Results and Discussion

$[\text{Ir}(\text{ppy})_2(\text{bpy})]^+$ and $[\text{Rh}(\text{bpy})_3]^{3+}$ -exchanged acidic resin was obtained by stirring a suspension of a commercially available resin (Amberlite 200CNa = resin **1**) in H_2O /acetonitrile (9:1) containing both Ir and Rh complexes for 2 days at 343 K. Prior to ion exchange, resins were crushed by ball milling (600 rpm for 10 min). Several samples with different loadings (Ir:Rh = 1:1, Ir + Rh = 0.5, 1.0, and 2.0 wt.%) and different molar ratios (Ir + Rh = 1.0 wt.%, Ir:Rh = 1:0, 10:1, 4:1, 2:1, 1:1, 1:2, and 0:1) were prepared. The Ir and Rh contents were measured by inductively coupled plasma (ICP) analysis.

As shown in inset of Figure 2, the UV/Vis spectrum of the $[\text{Ir}(\text{ppy})_2(\text{bpy})]^+$ complex in acetonitrile exhibits intense absorption bands in the high energy region ($\lambda < 300$ nm), as-

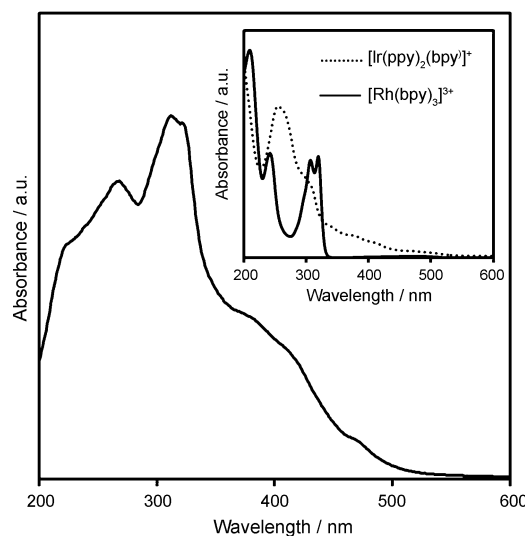


Figure 2. UV/Vis spectrum of Ir-Rh/resin **1**. The inset shows the UV/Vis spectra of $[\text{Ir}(\text{ppy})_2(\text{bpy})]^+$ and $[\text{Rh}(\text{bpy})_3]^{3+}$ solutions in acetonitrile.

signed to the spin-allowed singlet ligand-centered transition for ppy and bpy ligands (^1LC , $\pi-\pi^*$), and moderate low-energy bands ranging from 350 to 400 nm, ascribed to the spin-allowed singlet MLCT transition, and weaker absorption tails ranging to 500 nm that are attributed to a mixture of spin-forbidden ^3LC and $^3\text{MLCT}$ transitions.^[13] The spectrum of the $[\text{Rh}(\text{bpy})_3]^{3+}$ complex in acetonitrile exhibits absorption bands assigned to the ^1LC transition for bpy ligands at around 300 nm, while no absorption is observed in the visible region. The spectrum of the Ir-Rh/resin **1** (Ir:Rh =

1:1, Ir+Rh=1.0 wt. %) contains the absorption bands observed for the free Ir and Rh complexes, suggesting that both complexes can easily diffuse within the macroreticular resin matrix to lead to a homogeneous distribution. The absorption intensity in the visible region ($\lambda > 400$ nm) increased with increasing the amount of Ir complex (data not shown).

X-ray absorption measurements were conducted to elucidate the electronic structure and chemical environment of the exchanged metal complexes. Figure 3A shows normalized X-ray absorption near-edge structure (XANES) spectra

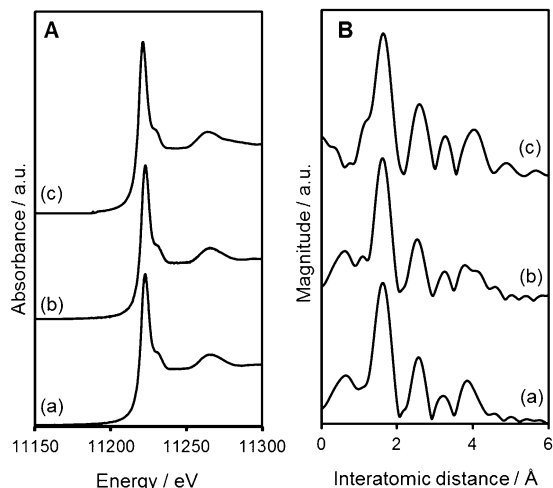


Figure 3. (A) Ir L_{III} -edge XANES spectra and (B) FT-EXAFS spectra of $[\text{Ir}(\text{ppy})_2(\text{bpy})]^+$ (a), Ir-Rh/resin **1** (b), and recovered Ir-Rh/resin **1** (c).

at the Ir L_{III} -edge of the $[\text{Ir}(\text{ppy})_2(\text{bpy})]^+$ complex and Ir-Rh/resin **1** (Ir:Rh = 1:1, Ir+Rh = 1.0 wt. %). The white line at around 11222 eV assigned to the allowed $2p \rightarrow nd$ transition is intensified with an increase in the d-band vacancies as a result of oxidation.^[14] Thus, the white line absorption peaks of oxidized Ir species are more intense than those of reduced species. Figure 3A reveals that the intensity of the exchanged resin sample almost matches that of the free complex. In the Fourier transformations (FT) of the Ir L_{III} -edge X-ray absorption fine structure (EXAFS) spectra (Figure 3B), a strong peak attributable to Ir–N and/or Ir–C bonds is observed at around 1.5 Å in addition to a small second shell at about 2.4 Å, which is assigned to neighboring carbon atoms. This result verifies a tridentate binding structure for the Ir^{III} center in octahedral coordination. Figure 4 shows XANES and FT-EXAFS spectra of the $[\text{Rh}(\text{bpy})_3]^{3+}$ complex and Ir-Rh/resin **1** (Ir:Rh = 1:1, Ir+Rh = 1.0 wt. %) at the Rh K-edge. The Rh K-edge XANES spectrum of Ir-Rh/resin **1** is quite similar to that observed for the free $[\text{Rh}(\text{bpy})_3]^{3+}$ complex. The FT-EXAFS spectra show a strong peak attributable to Ru–N bonds at around 1.5 Å and a small second shell assigned to neighboring carbon atoms at about 2.5 Å. Together, these data confirm a bidentate binding structure in the Rh^{II} oxidation state. All XAFS data

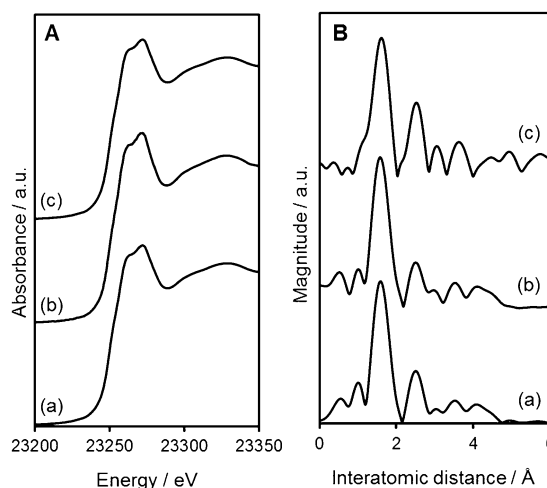


Figure 4. (A) Rh K-edge XANES spectra and (B) FT-EXAFS spectra of $[\text{Rh}(\text{bpy})_3]^{3+}$ (a), Ir-Rh/resin **1** (b), and recovered Ir-Rh/resin **1** (c).

reveal that the exchanged metal complexes within the macroreticular resin matrix retain their original structures.

The emission spectra are dependent on the ligand field strength, the redox properties of the metal and ligands, and the intrinsic properties of the ligands.^[15] Therefore, a slight change in the surroundings of the Ir complex significantly influences the orbital nature of the excited state. The inset in Figure 5 shows the photoluminescence spectra of a solution of the $[\text{Ir}(\text{ppy})_2(\text{bpy})]^+$ complex in acetonitrile at room temperature and 77 K upon excitation at 370 nm. The $[\text{Ir}(\text{ppy})_2(\text{bpy})]^+$ complex exhibits phosphorescence emission at around 585 nm at room temperature, which is mainly attributable to the $^3\text{MLCT}$ transition.^[16] Upon cooling to 77 K, the emission maximum was shifted to about 570 nm and can be principally assigned to the ^3LC level in a higher triplet state rather than $^3\text{MLCT}$. This significant blue-shift can be

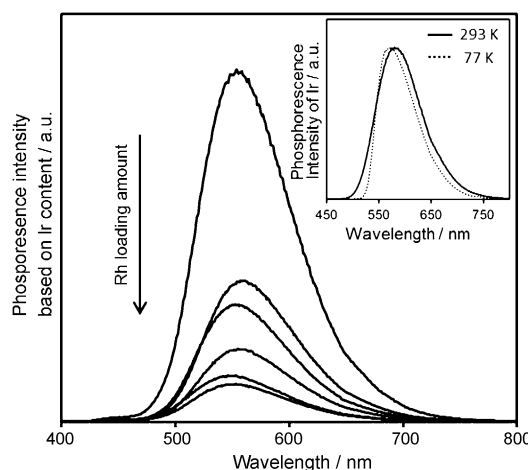
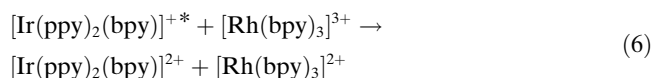


Figure 5. Photoluminescence spectra of Ir-Rh/resins **1** of different Ir/Rh molar ratios at room temperature ($\lambda_{\text{ex}} = 370$ nm). The inset shows the photoluminescence spectra of $[\text{Ir}(\text{ppy})_2(\text{bpy})]^+$ in acetonitrile at room temperature and at 77 K ($\lambda_{\text{ex}} = 370$ nm).

simply explained by the efficient quenching of thermally activated deactivation processes at 77 K, so that luminescence from ³LC levels can incidentally occur.^[16–17] The asymmetry of the emission band at 77 K reveals a skewing of the emission maximum toward shorter wavelengths. This behavior originates from the poorly resolved vibronic structure and is analogous to that of Pt^{II} polypyridyl complexes.^[18]

The tendency is different for Ir-Rh-resin **1**, where phosphorescence emission of the powdered sample is blue-shifted relative to that of the free complex in acetonitrile at room temperature, with a maximum near 550 nm (Figure 5). Furthermore, the shift toward shorter wavelength was small (~3 nm) upon switching from room temperature to 77 K (data not shown). No significant emission due to the [Rh(bpy)₃]³⁺ complex was observed in this wavelength region. It is likely that the vibrational relaxation of the triplet MLCT excited states in the Ir-Rh-resin **1** is inhibited by the unique surroundings within the resin matrix. Thus, phosphorescence emission from the higher ³MLCT state mainly occurs, receiving substantial contribution from close-lying ³MLCT levels, thereby resulting in a blue shift in the emission spectra. This explanation agrees with the so-called “rigidochromism” originally termed by Wrington and Morse.^[19] Similar phenomena have also been observed for the [Ir(ppy)₂(bpy)]⁺ complex intercalated in layered silicate materials.^[20] Notably, the peak intensity reaches a maximum with the Ir/resin **1** (i.e., without the Rh complex) and increases in the Rh loading resulted in a significant decrease in emission intensity. This result provides clear evidence that both Ir and Rh complexes within the macroreticular resin matrix are present within short distances that allows for a cooperative action, so that the excited state of the Ir complex undergoes an efficient oxidative quenching by the Rh complex following Equation (6).^[7b]



Ir-Rh resin catalysts were also prepared from other commercially available resins (Amberlite, Rohm and Haas). The characteristics of the resins used are summarized in Table 1. Resins Amberlite 200C Na (resin **1**), Amberlyst 15DRY (resin **2**), and Amberlyst 16WET (resin **3**) are strongly acidic, while Amberlite FPC3500 (resin **4**) is weakly acidic. Resin 200C Na and 16WET have a higher water-absorption capacity (swelling property) than 15DRY. Through ICP analysis we determined that the Ir and Rh complexes were easily attached to the resins at the same level of loading (Ir:Rh = 1:1, Ir + Rh = 1.0 wt. %). All of the resins had moderate BET-specific surface areas of approximately 45 m² g⁻¹. In separate experiments, the deposition of metal complexes

Table 1. Textural properties of resin-supported Ir/Rh catalysts.

Catalyst	Resin ^[a]	Functional group	Exchange capacity [mequiv mL ⁻¹]	Property	Water absorption capacity [%]
Ir-Rh/resin 1	200C Na	-SO ₃ Na	≥ 1.8	strongly acidic	46–51
Ir-Rh/resin 2	15DRY	-SO ₃ H	≥ 2.6	strongly acidic	1–2
Ir-Rh/resin 3	16WET	-SO ₃ H	≥ 1.7	strongly acidic	52–58
Ir-Rh/resin 2	FPC3500	-COOH	≥ 2.0	weakly acidic	60–70

[a] Styrenic matrix except for resin **4** (acrylic).

to anion-exchange resins possessing basic groups within its macroreticular matrices was unsuccessful. The potential photocatalytic activity of the Ir-Rh/resins for H₂ production was then evaluated under irradiation with visible light (λ > 420 nm) in H₂O/acetonitrile (9:1) containing 0.6 M triethylamine (TEA) as a sacrificial reagent. Figure 6A shows the time course of the H₂ production using various resin cata-

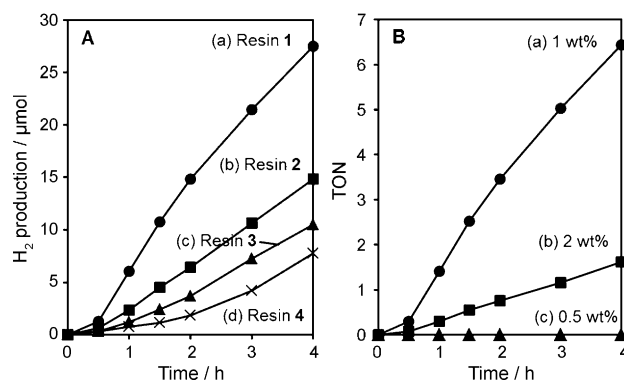


Figure 6. (A) Effect of resin (Ir:Rh = 1:1, Ir + Rh = 1.0 wt. %) on photocatalytic H₂ production. (B) Effect of the metal loading amount in Ir-Rh/resin **1** (Ir:Rh = 1:1) on the TON for photocatalytic H₂ production. λ_{ex} > 420 nm.

lysts. No reaction was observed in the dark in the presence of the photocatalyst or in the absence of TEA under light irradiation. Moreover, H₂ production did not occur to any significant extent in the presence of resin **1** without metal complexes under identical reaction conditions. It should be noted that the photocatalytic activity of the used resins varied significantly, and resin **1** with a strong acidity as well as high water-absorption capacity was found to have the highest activity. The effect of metal loading amounts were also investigated using Ir-Rh/resin **1** (Ir:Rh = 1:1) with different metal loading amounts (Ir + Rh = 0.5, 1.0, and 2.0 wt. %, Figure 6B). The metal loading amount within resins was controlled by changing the initial ratio of resin to metal complexes in the slurry. Almost no reaction occurred at 0.5 wt% loading. The TON for H₂ formation reached a maximum at 1.0 wt. %, while a further increase to 2.0 wt. % loading decreased the photocatalytic activity. This decrease may be ascribed to a filter effect. The efficient formation of H₂ with a small amount of metal complexes is valuable as the consumption of expensive metals is reduced.

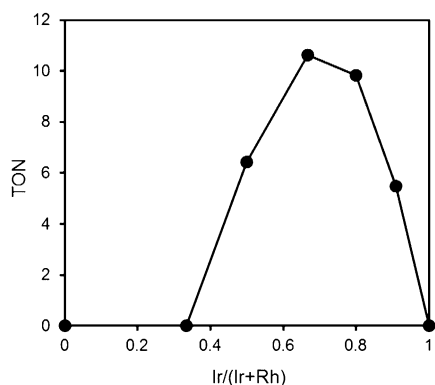


Figure 7. Effect of the molar ratio of Ir/Rh complexes in Ir-Rh/resin **1** on the TON for photocatalytic H₂ production ($\lambda_{\text{exc}} > 420$ nm).

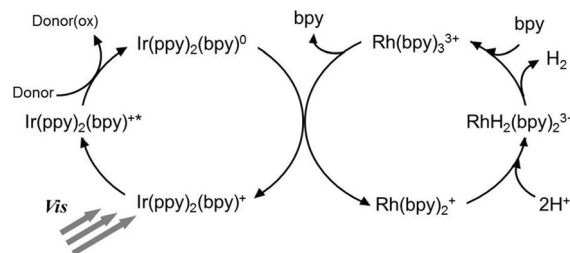
The influence of the molar ratio of the Ir complex (photosensitizer) to the Rh complex (proton reduction catalyst) within the resin was also explored, as shown in Figure 7. Both Ir and Rh complexes were indispensable for H₂ production; no reaction occurred in the absence of either the Ir or the Rh complex. The maximal turnover number (TON) was obtained at Ir/(Ir+Rh)=0.67, which corresponds to Ir:Rh=2:1. In simple terms, this reaction is facilitated by a direct electron transfer from the photosensitizer to the proton reduction catalyst without an electron mediator. Our results indicate that the electron-transfer step is crucial and may be a rate-determining step.

Considering the aforementioned photocatalytic results, different types of sacrificial reagents (SRs) were studied. TEA was found to be most effective among the SRs investigated. The use of MeOH, EtOH, HCOOH, and CH₃COOH instead of TEA resulted in no activity. The present Ir-Rh system has an even greater influence on the photocatalytic activity than the traditional Ru-based system because the former contains a reductive quenching step of the excited-state photosensitizer Ir complex by the SR, as mentioned below. Actually, it has been reported that the quenching constant of [Ir(ppy)₂(bpy)]⁺ for TEA ($k_q = 1.2 \times 10^8 \text{ M}^{-1} \text{ s}^{-1}$) is larger than that for triethanolamine (TEOA, $k_q = 5.4 \times 10^6 \text{ M}^{-1} \text{ s}^{-1}$) as assessed by using laser flash photolysis.^[7b]

Whether H₂ production occurs on colloidal metal or the molecular complex is controversial.^[21] In our experiments we have found that the XAFS spectrum of the recovered Ir-Rh/resin **1** after the photocatalytic reaction is identical to that of the fresh catalyst (Figures 3 and 4, compare curves b and c), thus indicating that no changes occurred in the electronic configuration and local structures. Moreover, the recovered Ir-Rh/resin **1** retains its original photocatalytic activity, thereby suggesting that the photoreaction proceeds on the molecular species exchanged within the macroporous space of the resin. These data support the notion that the molecular species rather than the colloidal form are participate in the catalysis.

As aforementioned, the classical molecule-based photocatalytic H₂ production system consists of multiple components including a PS (Ru(bpy)₃²⁺), an ER (methylviologen),

a WRC (colloidal Pt), and an SR. The electron relay step is generally crucial to the success of a photocatalytic system; an efficient ER oxidatively quenches the excited PS, thereby allowing charge separation at the expense of simplicity. It is noteworthy that the present photocatalyst capable of visible-light photosensitization associated with the ³LC and ³MLCT excited states of the Ir complex and hydrogenic activation of the Rh complex produces H₂ without an electron relay. A possible reaction pathway is illustrated in Scheme 1.^[7b] Firstly, the excited state of the [Ir(ppy)₂(bpy)]⁺ is reductively quenched by TEA (SR) to produce [Ir(ppy)₂(bpy)]⁰. Sec-



Scheme 1. A possible reaction pathway for photocatalytic H₂ production using the Ir-Rh/resin.

ondly, the activated reduced Ir species directly deliver reducing equivalents to Rh WRC, and finally produce H₂ via a reductive elimination from the Rh dihydride species in a homolytic unimolecular pathway. Although the oxidation state of the active WRC is unclear, [Rh(bpy)₂]⁺ generated by two consecutive reductions with the activated reduced Ir species and labilization of the bpy ligand is postulated as one of the possible active species.^[22] It is important to note that the first reductive quenching step is distinct from the traditional system involving [Ru(bpy)₃]²⁺, which undergoes oxidative quenching by the ER to generate [Ru(bpy)₃]³⁺. Since the LUMO (lowest singly unoccupied molecular orbital) of [Ir(ppy)₂(bpy)]⁺ involves both d orbitals of the Ir center and the π orbitals of the ppy ligands, the reductive electron transfer reaction and increase in the spatial charge separation in the excited state may be facilitated. In the present catalytic system, a maximal TON was obtained at Ir:Rh=2:1, which supports the above mechanism involving two consecutive reductions of the high-valent Rh species by the reduced Ir species and further implies that the electron transfer step may be a rate-determining step. The macroporous environment of the resin can provide the existence of both Ir and Rh complexes in close proximity, which assists the cooperative action of adjacent complexes, thus ultimately enhancing the photooxidation activity.

Conclusions

Ion exchange of photosensitizer iridium(III) and proton reduction catalyst rhodium(III) complexes within a macroporous acidic resin provides a new type of photocatalyst with

unique photoluminescent properties as well as photocatalytic activities. Photoluminescence emission due to the Ir complex of the Ir-Rh/resin was significantly blue-shifted relative to that of the free complex in acetonitrile at room temperature because of the rigidochromism effect. The excited state of the Ir complex within the macroreticular resin undergoes an efficient oxidative quenching by an adjacent Rh complex, and the peak intensity therefore decreased with increasing the Rh loading amount. The Ir-Rh/resin catalyst behaves as a recyclable heterogeneous photocatalyst for H₂ production in aqueous solution, in which direct electron transfer from Ir to Rh occurs in the absence of a mediator. Further studies are currently ongoing to develop novel photocatalysts with enhanced activity and durability.

Experimental Section

Synthesis of [Ir(ppy)₂(bpy)]PF₆²³⁾

A mixture of 2-phenylpyridine (5.3 mmol) and IrCl₃·3H₂O (2.1 mmol) in 2-methoxyethanol/water (5:1) was stirred under reflux conditions (393 K) for 15 h under an Ar atmosphere. The resulting precipitate was filtered off, washed with water and Et₂O (100 mL each), and dried to yield the product, [(CN)₂Ir-μ-Cl]₂. The obtained dichloro-bridged dimer (0.9 mmol) was then reacted with 2,2'-bipyridine (1.9 mmol) in ethylene glycol (50 mL) for 15 h under reflux (423 K) under constant stirring. After cooling to room temperature, the mixture was transferred to a separatory funnel with water (3×50 mL) and washed with Et₂O (3×50 mL). The aqueous layer was heated to remove residual Et₂O. The vessel was then placed on ice, and 10 mL of aqueous ammonium hexafluorophosphate (5.0 g in 20 mL of deionized water) was slowly added to the reaction mixture, yielding [Ir(ppy)₂(bpy)]PF₆ as a yellow precipitate (1.20 g, 71 % yield). Structural identification was performed by ¹H NMR spectroscopy.

Synthesis of [Rh(bpy)₃](PF₆)₃²⁴⁾

RhCl₃·2H₂O (2.0 mmol) and 2,2'-bipyridine (7.0 mmol) was added to EtOH (20 mL) and H₂O (20 mL), and the mixture was heated at 353 K. After 15 min, 2.0 mL of a 2 M solution of hydrazine in EtOH/H₂O (1:1) was added, and the mixture was heated for an additional hour at 353 K. NH₄PF₆ (1.0 g in 2 mL of H₂O) was added, and the reaction mixture was concentrated to about 10 mL by evaporation. The resulting solids were filtered off, washed with water (20 mL), and dried overnight to afford [Rh(bpy)₃](PF₆)₃ as white crystals (1.31 g, 65 % yield). Structural identification was performed by ¹H NMR spectroscopy.

Synthesis of Photocatalyst

Several Ir/Rh catalysts were prepared from different commercially available resins (Amberlite, Rohm and Haas). Prior to their use, resins were crushed by a ball mill (600 rpm for 10 min). A solution of [Ir(ppy)₂(bpy)]PF₆ (0.027 mmol, 21.5 mg) and [Rh(bpy)₃](PF₆)₃ (0.027 mmol, 27.3 mg) in acetonitrile (10 mL) was added to an aqueous suspension (90 mL) containing the resin (0.5 g), and the mixture was stirred at 343 K for 48 h. The resin was then filtered off, washed repeatedly with distilled water/acetonitrile (1:1, 200 mL) and dried overnight to afford a Ir-Rh/resin (Ir:Rh=1:1). Other samples with different metal loadings were also prepared by varying the initial concentration of complexes. The metal loadings were determined by inductively coupled plasma (ICP) analysis.

Characterization

BET surface area measurements were performed using a BEL-SORP max (Bel Japan, Inc.) instrument at 77 K. The sample was degassed in vacuum at 353 K for 24 h prior to data collection. UV/Vis diffuse reflectance spectra of powdered samples were collected using a Shimadzu UV-

2450 spectrophotometer. The reference was BaSO₄, and the absorption spectra were obtained using the Kubelka-Munk function. Inductively coupled plasma-optical emission spectrometry (ICP-OES) measurements were performed using a Nippon Jarrell-Ash ICAP-575 Mark II instrument. Photoluminescence measurements were carried out on a fluorolog-3 spectrofluorometer (Horiba). Ir L_{III}-edge and Rh K-edge XAFS spectra were recorded using a fluorescence-yield collection technique at the beam line 01B1 station with an attached Si (311) monochromator at SPring-8, JASRI, Harima, Japan. The EXAFS data were normalized by fitting the background absorption coefficient around the energy region higher than that of the edge of about 35–50 eV, with smooth absorption of an isolated atom. The EXAFS data were examined using the Rigaku EXAFS analysis program. Fourier transformation (FT) of *k*³-weighted normalized EXAFS data was performed over the 3.5 Å < *k*/Å⁻¹ < 11 Å range to obtain the radial structure function.

Photocatalytic H₂ Production

The powdered Ir-Rh/resin catalyst (50 mg), H₂O/acetonitrile (10 mL, 9:1), and triethylamine (TEA, 0.6 mL) were introduced into a reaction vessel that was then sealed with a rubber septum. The resulting mixture was bubbled with Ar for 15 min in the dark. Subsequently, the sample was irradiated from the side using a Xe lamp (500 W; SAN-EI ELECTRIC CO., Ltd. XEF-501S) through the glass filter (λ > 420 nm) with magnetic stirring at ambient pressure and temperature. The reaction progress was monitored using a Shimadzu GC-14B gas chromatograph equipped with a MSSA column.

Acknowledgements

This work was supported by the Grant-in-Aid for Scientific Research from the Ministry of Education Culture, Sports, Science and Technology of Japan (252892890). A part of this work was also performed under a management of 'Elements Strategy Initiative for Catalysts & Batteries (ESICB)' supported by MEXT. XAFS spectra were recorded using a fluorescence-yield collection technique at the beam line 01B1 station with an attached Si (311) monochromator at SPring-8, JASRI, Harima, Japan (prop. No. 2012A1061 and 2012B1058).

- [1] a) M. Grätzel, *Acc. Chem. Res.* **1981**, *14*, 376–384; b) N. S. Lewis, D. G. Nocera, *Proc. Natl. Acad. Sci. USA* **2006**, *103*, 15729–15735; c) A. J. Esswein, D. G. Nocera, *Chem. Rev.* **2007**, *107*, 4022–4047.
- [2] A. Fujishima, K. Honda, *Nature* **1972**, *238*, 37–38.
- [3] a) M. Grätzel, *Nature* **2001**, *414*, 338–344; b) H. Arakawa, K. Sayama, *Catal. Surv. Jpn.* **2000**, *4*, 75–80; c) K. Maeda, K. Domen, *J. Phys. Chem. C* **2007**, *111*, 7851–7861; d) A. Kudo, Y. Miseki, *Chem. Soc. Rev.* **2009**, *38*, 253–278.
- [4] a) L. L. Tinker, N. D. McDaniel, S. Bernhard, *J. Mater. Chem.* **2009**, *19*, 3328–3337; b) M. Wang, Y. Na, M. Gorlov, L. Sun, *Dalton Trans.* **2009**, 6458–6467; c) P. D. Tran, V. Artero, M. Fontecave, *Energy Environ. Sci.* **2010**, *3*, 727–747; d) H. Ozawa, K. Sakai, *Chem. Commun.* **2011**, *47*, 2227–2242.
- [5] A. Moradpour, E. Amouyal, P. Keller, H. Kagan, *Nouv. J. Chim.* **1978**, *2*, 547–549.
- [6] H. Ozawa, M.-a. Haga, K. Sakai, *J. Am. Chem. Soc.* **2006**, *128*, 4926–4927.
- [7] a) L. L. Tinker, N. D. McDaniel, P. N. Curtin, C. K. Smith, M. J. Ireland, S. Bernhard, *Chem. Eur. J.* **2007**, *13*, 8726–8732; b) E. D. Cline, S. E. Adamson, S. Bernhard, *Inorg. Chem.* **2008**, *47*, 10378–10388; c) Y.-J. Yuan, J.-Y. Zhang, Z.-T. Yu, J.-Y. Feng, W.-J. Luo, J.-H. Ye, Z.-G. Zou, *Inorg. Chem.* **2012**, *51*, 4123–4133.
- [8] N. E. Leadbeater, M. Marco, *Chem. Rev.* **2002**, *102*, 3217–3274.
- [9] C. A. McNamara, M. J. Dixon, M. Bradley, *Chem. Rev.* **2002**, *102*, 3275–3300.

- [10] a) K. Mori, A. Hanafusa, M. Che, H. Yamashita, *J. Phys. Chem. Lett.* **2010**, *1*, 1675–1678; b) K. Mori, M. Dojo, H. Yamashita, *ACS Catal.* **2013**, *3*, 1114–1119.
- [11] C. Ulbricht, B. Beyer, C. Friebe, A. Winter, U. S. Schubert, *Adv. Mater.* **2009**, *21*, 4418–4441.
- [12] N. Sutin, C. Creutz, E. Fujita, *Comments Inorg. Chem.* **1997**, *19*, 67–92.
- [13] M. G. Colombo, A. Hauser, H. U. Guedel, *Inorg. Chem.* **1993**, *32*, 3088–3092.
- [14] a) P. I. Ravikovitch, A. V. Neimark, *Langmuir* **2000**, *16*, 2419–2423; b) K. Mori, M. Tottori, K. Watanabe, M. Che, H. Yamashita, *J. Phys. Chem. C* **2011**, *115*, 21358–21362.
- [15] S. I. Gorelsky, E. S. Dodsworth, A. B. P. Lever, A. A. Vlcek, *Coord. Chem. Rev.* **1998**, *174*, 469–494.
- [16] S.-H. Wu, J.-W. Ling, S.-H. Lai, M.-J. Huang, C. H. Cheng, I. C. Chen, *J. Phys. Chem. A* **2010**, *114*, 10339–10344.
- [17] Y. Ohsawa, S. Sprouse, K. A. King, M. K. DeArmond, K. W. Hanck, R. J. Watts, *J. Phys. Chem.* **1987**, *91*, 1047–1054.
- [18] K. Wang, M.-a. Haga, H. Monjushiro, M. Akiba, Y. Sasaki, *Inorg. Chem.* **2000**, *39*, 4022–4028.
- [19] M. Wrighton, D. L. Morse, *J. Am. Chem. Soc.* **1974**, *96*, 998–1003.
- [20] D. Mochizuki, M. Sugiyama, M. M. Maitani, Y. Wada, *Eur. J. Inorg. Chem.* **2013**, *13*, 2324–2329.
- [21] a) P. Lei, M. Hedlund, R. Lomoth, H. Rensmo, O. Johansson, L. Hammarström, *J. Am. Chem. Soc.* **2008**, *130*, 26–27; b) K. Yamachi, S. Masaoka, K. Sakai, *J. Am. Chem. Soc.* **2009**, *131*, 8404–8406.
- [22] M. Kirch, J.-M. Lehn, J.-P. Sauvage, *Helv. Chim. Acta* **1979**, *62*, 1345–1384.
- [23] M. S. Lowry, J. I. Goldsmith, J. D. Slinker, R. Rohl, R. A. Pascal, G. G. Malliaras, S. Bernhard, *Chem. Mater.* **2005**, *17*, 5712–5719.
- [24] J. E. Hillis, M. K. DeArmond, *J. Lumin.* **1971**, *4*, 273–290.

Received: July 30, 2013
Published online: September 20, 2013